



Article

Degradation of Carbon Fiber-Reinforced Polymer Composites in Salt Water and Rapid Evaluation by Electrochemical Impedance Spectroscopy

Hanlu Zhang^{1,2,†}, Fabao Kong^{1,†}, Yuchao Dun³, Xueping Chen¹, Quankai Chen¹, Xuhui Zhao^{1,*} , Yuming Tang^{1,*}  and Yu Zuo¹

¹ Key Laboratory of Carbon Fiber and Functional Polymers, Ministry of Education, Beijing University of Chemical Technology, Beijing 100029, China

² Corrosion Protection and Materials Research Laboratory, No. 92228 of the People's Liberation Army, Beijing 100072, China

³ Aviation Key Laboratory of Science and Technology on Advanced Surface Engineering, AVIC Manufacturing Technology Institute, Beijing 100024, China

* Correspondence: xzhao@mail.buct.edu.cn (X.Z.); tangym@mail.buct.edu.cn (Y.T.)

† These authors contributed equally to this work.

Abstract: The electrochemical impedance spectroscopy and weight gain tests were performed on carbon fiber/vinyl ester and carbon fiber/bismaleimide composites in 3.5% NaCl solution to study the electrochemical and water absorption behaviors. The microstructure morphology and the flexural property of the composites in the long-term exposure process were analyzed with the scanning electron microscope and four-point bending tests. The results revealed that after long-time immersion (>200 d), the water absorption of the two composites is less than 0.5%. This has little effect on the microstructural integrity, only with slight damage on the fiber/resin interfaces, but results in a significant decrease (about 84%) in the composite flexural property. The variation of the water absorption percentage shows good consistency with that of the resin capacitance (Q_c) and is negatively related to the variation of the resin resistance (R_{po}) and the low-frequency impedance ($|Z|_{0.01\text{Hz}}$) of the composites. A good linear relationship exists between the variations of phase angles in the middle-frequency range (0.1–10 Hz) and the $|Z|_{0.01\text{Hz}}$. The phase angle at 10 Hz ($\theta_{10\text{Hz}}$) may be suggested as a suitable parameter to rapidly evaluate the performance of carbon fiber-reinforced polymer composites, just like for evaluating the protective performance of polymer-coated metals in the literature.

Keywords: carbon fiber-reinforced composite; vinyl resin; bismaleimide resin; EIS; evaluation



Citation: Zhang, H.; Kong, F.; Dun, Y.; Chen, X.; Chen, Q.; Zhao, X.; Tang, Y.; Zuo, Y. Degradation of Carbon Fiber-Reinforced Polymer Composites in Salt Water and Rapid Evaluation by Electrochemical Impedance Spectroscopy. *Materials* **2023**, *16*, 1676. <https://doi.org/10.3390/ma16041676>

Academic Editor: Magdalena Sobiesiak

Received: 16 January 2023

Revised: 8 February 2023

Accepted: 14 February 2023

Published: 17 February 2023



Copyright: © 2023 by the authors. Licensee MDPI, Basel, Switzerland. This article is an open access article distributed under the terms and conditions of the Creative Commons Attribution (CC BY) license (<https://creativecommons.org/licenses/by/4.0/>).

1. Introduction

Because of their high specific strength, high stiffness, and very good corrosion resistance, carbon fiber reinforced polymers (CFRP) have been widely used in aircraft, aerospace, automotive, civil, and electronics industries. Compared with metallic engineering materials, carbon fiber-reinforced composites have much better corrosion resistance. However, long-time immersion in aggressive service environments or galvanic coupling with engineering metals (steels and aluminum alloys, etc.) would lead to a decrease in the stability or even accelerate the degradation of the composites [1–5].

Carbon fiber/vinyl ester and carbon fiber/epoxy systems are often chosen because of their easy processing and potential durability considerations [6]. Compared with epoxy resin, vinyl ester resin has a relatively low cost and superior chemical stability in salt water, so more and more vinyl ester-based carbon-reinforced composites have been used as structural materials in marine environments [6–8]. Marouani et al. studied the durability of carbon fiber-reinforced composites with epoxy and vinyl ester matrixes in two kinds

of aging conditions [6]. Their research results showed that vinyl ester composites have better hydrolysis resistance, even at elevated temperatures. Kootsookos et al. comparatively studied the chemical stability of vinyl ester-based and polyester-based carbon fiber composites [7]. They concluded that with the amounts of water absorption increasing, some chemical degradation occurs to the vinyl ester-based composite, but to a much lower extent than that for the polyester-based carbon fiber composite. Afshar et al. studied the flexural property variation of the carbon fiber vinyl ester composite in indoor and outdoor conditions and discussed the correlation between long-term outdoor exposure and laboratory conditions [8]. Alias et al. investigated the damage to the carbon fiber vinyl ester composite from cathodic polarization and concluded that two types of damage, blistering and dissolution, occurred because of the galvanic interactions and seawater immersion [9].

Bismaleimide (BMI) resin matrix carbon fiber reinforced composites possess very good thermal stability and mechanical properties; thus, they are currently being used as structural materials for military and civilian aircraft [10,11]. Akay et al. studied the effects of long-term exposure at high temperatures on the interlaminar shear and impact performance of a carbon fiber bismaleimide composite [11]. Bao et al. studied the moisture absorption and hygrothermal aging of a bismaleimide resin-based carbon fiber composite material, and the results indicated that the composites present a two-stage diffusion behavior [12]. Li et al. investigated the mechanical properties of T700 carbon fiber-reinforced bismaleimide composites under hygrothermal conditions and discussed the synergistic effect of moisture absorption and temperature on the decrease in mechanical properties [13].

In carbon fiber-reinforced polymer composites, the integrity of the interface between the carbon fiber and the matrix is usually evaluated macroscopically via the interlaminar shear strength (ILSS) or the interfacial shear strength (IFSS) [4]. However, these are destructive methods and are not suitable for the long-term monitoring of composite properties. Electrochemical impedance spectroscopy (EIS) is a non-destructive electrochemical technique that has been widely used in the field of polymeric coatings for studying the coating degradation and monitoring the corrosion process at the metal-coating interface. Through spectra analysis or the use of equivalent circuit modeling, the delamination of the coating from the substrate can be quantitatively measured, and the coating failure can be predicted. Since carbon fibers possess electrical conductivity, the EIS technique could be applied to study the property variation of carbon fiber-reinforced composites [9,14]. Alias et al. and Kaushik et al. measured the impedance spectra of carbon fiber/vinyl ester composite and carbon fiber/epoxy composite in 3.5% NaCl solution and analyzed the impedance data by the equivalent circuit models, which are commonly used for coated metals study [15,16]. It was suggested that the resistance of polymer matrix (R_{po}) determined from the circuit models might offer a damage-monitoring method for carbon fiber composite materials. Taylor et al. studied the impedance spectra of a graphite fiber/bismaleimide composite under conditions of applied polarization and coupled with metals in 0.6 M NaCl solution [17]. They suggested that EIS might be a sensitive method for monitoring the changes in surface morphology and chemistry of carbon fiber reinforced composites, especially since the phase angle is very sensitive in characterizing the changes in the composite. Mueller et al. investigated the damage behavior of carbon fiber-reinforced polyetheretherketone composites coupled with titanium and stainless steel in a simulated body fluid by polarization and EIS techniques [18]. They pointed out that monitoring electrochemical parameters offers the possibility to analyze changes in the properties of carbon fiber composites. Zhang et al. studied the electrochemical behaviors of carbon fiber-reinforced polymers with epoxy and nylon matrix in simulated auto industry solution by EIS method and analyzed the influence of the microstructures and defects in the surface polymer layers on the electrochemical performance of the composites [19,20].

The conventional EIS analysis is based on the analysis of the impedance spectra to obtain the impedance parameters which can reflect the performance of the coating. It is tedious work and not suitable for field tests. The impedance modulus at low-frequency ($|Z|_{0.01\text{Hz}}$) is generally recognized for estimating the protectiveness of polymer coatings.

Usually, the higher the value of $|Z|_{0.01\text{Hz}}$, the better the protection performance of the polymer coatings possess [21]. In order to quickly evaluate the coating performance, some investigators suggested several methods based on the EIS technique, which could avoid fitting and analyzing complex impedance spectra to some extent [22–25]. Among them, the breakpoint frequency (f_b) method proposed by Haruyama et al. has attracted the attention of many investigators [22], where f_b is the frequency at which the phase angle equals 45° , which can be used to estimate the extent of delamination area at the interface between coating and metal without the measurement in the low-frequency region. In our previous studies [26,27], the measurement of the phase angles in middle-frequency (such as 10 Hz) was proposed for evaluating the protective performance of organic coatings because the variation of the phase angles in middle-frequency was found to follow a similar trend to that of the low-frequency impedance ($|Z|_{0.01\text{Hz}}$) for many organic coating systems. Since the measurement of the phase angles in the middle-frequency domain takes a very short time, it is very suitable for rapid testing and evaluation in field applications. Some researchers applied the variation of phase angle at 10 Hz to evaluate the performance of polymer coatings and suggested it can be used as a fast approach for monitoring the degradation process of the polymer coating on a metal substrate [28–33]. However, no work has currently been reported about the applicability of the phase angle method in evaluating the performance of carbon fiber-reinforced polymer composites.

In this work, two kinds of carbon fiber-reinforced polymer composites (a carbon fiber/vinyl ester composite and a carbon fiber/bismaleimide composite) were selected to be the research objects. The EIS technique and weight gain test, combined with a four-point bending test and scanning electron microscopy observation, were employed to study the degradation characteristic of the composites during long-time immersion (>200 d) in 3.5% NaCl solution. The impedance parameters and their relationship to the water adsorption behavior of the composites were emphatically analyzed. Based on these, the correlation between variations of the phase angles in the middle-frequency range and the $|Z|_{0.01\text{Hz}}$ during the degradation process of the composites was discussed. The objective is to provide a rapid evaluation method suitable for monitoring the structural integrity and performance of carbon fiber-reinforced polymer composites.

2. Experimental

2.1. Materials and Preparation

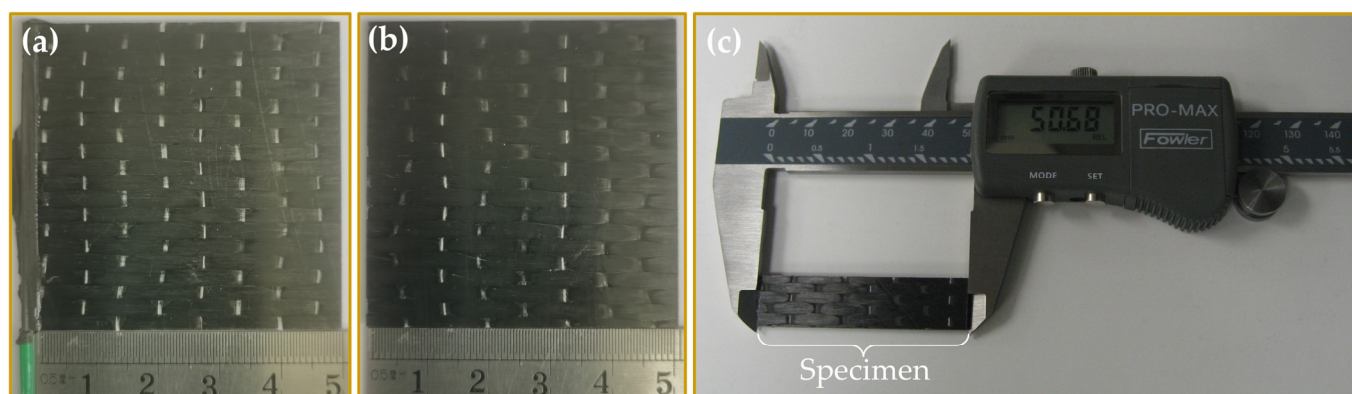
Because carbon fiber/vinyl ester-reinforced composites (CF/VE) have been widely used as structural materials in marine environments due to their relatively low cost and superior chemical stability, and carbon fiber/bismaleimide-reinforced composites (CF/BMI) have very good thermal stability and mechanical properties. Thus, the CF/VE and CF/BMI composite materials were selected in this work as the study materials; both are unidirectional carbon fiber-reinforced polymer composites.

In the CF/VE composite, a vinyl ester resin (Derakane MOMENTUM 411-350) was the matrix, which was catalyzed and promoted with methylethylketone peroxide and 6% cobalt naphthenate in the amounts of 1 phr and 0.05 phr, respectively, and T700 carbon fibers (Toray, Japan) coated with type FOE sizing was used as reinforcement. The composite was fabricated in the VARTM process at ambient temperature and then post-cured at 120°C for 2 h. The carbon fiber volume fraction in the composite was about 60%. Some of the cured plates were cut into $50.8 \times 50.8 \times 1 \text{ mm}^3$ specimens for weight gain and EIS tests and some $140 \times 20 \times 1 \text{ mm}^3$ specimens for a four-point bending test. In the CF/BMI composite, a 5428 bismaleimide resin (developed by Beijing Institute of Aeronautical Materials) with high toughness was the matrix, and T700 carbon fibers (Avic Composite Materials Co. Ltd., Beijing, China) coated with type FOE sizing was reinforcement. The composite was fabricated in the high-temperature resin transfer molding process. The carbon fiber volume fraction in the composite was about 55%. The cured CF/BMI composite plates had the same length and width as CF/VE CF/BMI with a 2 mm thickness. Table 1 shows the composition of these two composite materials.

Table 1. The composition of the carbon fiber reinforced composite materials.

Sample	Matrix	Reinforcement and Volume Fraction
CF/VE	Vinyl ester resin	T700 carbon fiber (60%)
CF/BMI	5428 Bismaleimide resin	T700 carbon fiber (55%)

For the EIS test, some specimens were prepared as working electrodes. The preparation method is as follows [34]. One side of the specimen, which was perpendicular to the carbon fibers' direction, was polished with sandpapers to expose the fibers. Then, an electrical connection was made using a nickel print coating (GC Electronics #22-207) to connect a copper wire to the side of the composite with exposed carbon fiber ends. After 24 h, an epoxy resin was applied to seal and fix the nickel print coating and the copper wire to the specimen. The other three edges of the specimen were also sealed by the epoxy resin and cured for 6 h prior to immersion. Figure 1 presents the macroscopic specimens for the EIS test, weight gain test, and mechanical property test.

**Figure 1.** The macroscopic specimens used for (a) EIS test; (b) weight gain test; (c) mechanical property test.

2.2. Measurements

Specimens were exposed to 3.5% NaCl solution in the open circuit potential state at ambient temperature. The EIS, weight gain, four-point bending, and scanning electronic microscopy (SEM) measurements were carried out periodically for the specimens.

The EIS test was performed using a PARSTAT 2273 instrument (Princeton, NJ, USA). A 5 mV perturbation was applied with a 10^5 Hz– 10^{-2} Hz scanning frequency range, and 30 frequencies were adopted. A three-electrode system was employed, in which the reference electrode was a saturated calomel electrode (SCE), the counter electrode was a platinum wire, and the composite specimen was the working electrode with 10 cm² exposed testing area. The test was carried out at an ambient temperature, and the number of parallel specimens was three. The data were fitted by the Zsimpwin Software (V 3.50).

The weight of the specimens before and after immersion in 3.5% NaCl solution for different periods was measured by an analytical balance (YP2003, Shanghai Yueping Science Instrument, Shanghai, China). The original specimen mass was recorded as m_0 . The specimen was withdrawn from the solution at regular intervals, washed and cleaned with deionized water, then carefully wiped dry with a paper towel to remove surface moisture and weighed. The mass of the specimen after a given immersion time was recorded as m_t . The percentage mass change ($M/\%_t$) of the specimen was calculated by Formula (1):

$$M/\%_t = \frac{m_t - m_0}{m_0} \quad (1)$$

The four-point bending test was performed by an MTS Insight 50 Universal Testing Machine (INSTRON-1121, INSTRON, Norwood, MA, USA) according to ASTM D6272-02

standard. Prior to the test, the specimen was withdrawn from immersion and carefully wiped dry with a paper towel. The applied crosshead speed was 1.5 mm/min. Five specimens were tested for each condition, and the mean value of flexural modulus (E_f) was determined by Formula (2). Where m is the gradient of the linear portion of the load–displacement curve, w and h are specimen width (20 mm) and thickness (1 mm), respectively, and L is the support span length (39 mm).

$$E_f = \frac{0.17L^3m}{wh^3} \quad (\text{GPa}) \quad (2)$$

The morphological structure of the composite specimen was characterized by a scanning electronic microscope (Hitachi S4700, Tokyo, Japan). The chemical element analysis was performed with energy disperse spectroscopy (EDS) (QUANTAX 70, BRUKER, Berlin, Germany). Before the SEM test, the specimen was cleaned, wiped dry, and sprayed with gold powder.

3. Results and Discussion

3.1. EIS Spectra of T700/VE Composite in 3.5% NaCl Solution

Figure 2 shows the Bode magnitude and phase angle plots of EIS spectra for the T700/VE composite specimen in 3.5% NaCl solution. After long-time immersion (205 d), there is no big change in the plots. At the start of exposure (5 min), the low-frequency impedance at 0.01 Hz ($|Z|_{0.01\text{Hz}}$) is $5.0 \times 10^6 \Omega \text{ cm}^2$, and the phase angle values approach 80 degrees in a wide frequency range (<100 Hz), which exhibits that the impedance response is very capacitive and the composite presents little conductivity [17,18]. As exposure progressed, the phase angle values in low and middle frequencies (<10 Hz) decreased slightly, indicating a gradually increasing ionic conductivity of the composite, possibly due to the slow penetration of electrolyte through the polymer matrix [16]. After 205 d, the value of $|Z|_{0.01\text{Hz}}$ is about $1.0 \times 10^6 \Omega \text{ cm}^2$ with a decrease in less than one order of magnitude compared with the original value, and the phase angle at 0.01 Hz is higher than 54 degrees. These demonstrate that the T700/VE composite has very good chemical stability in salt water at open circuit potential conditions, which verifies the results in the literature [6–8].

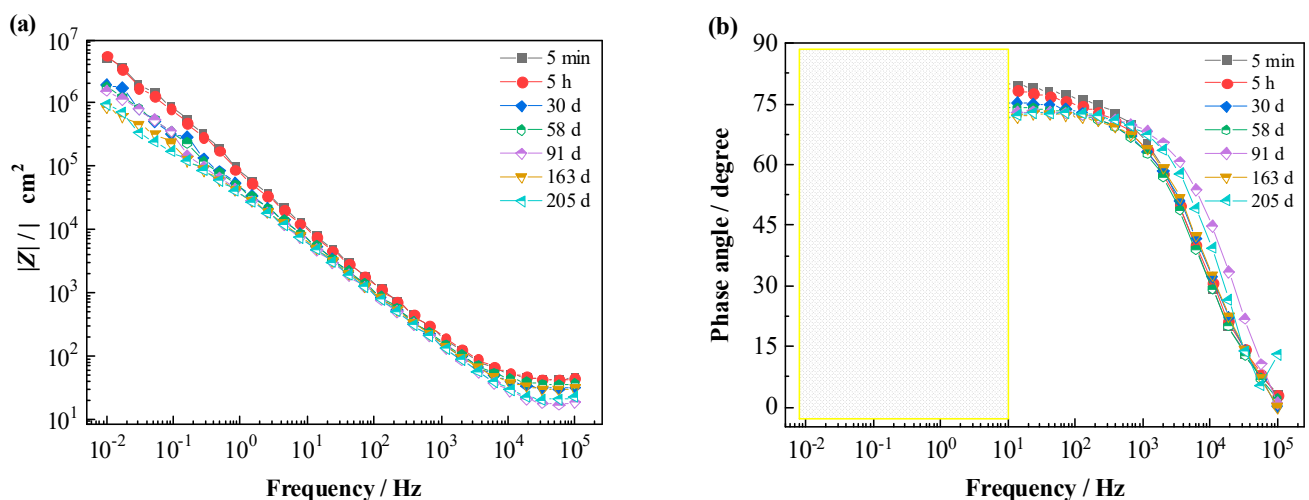


Figure 2. EIS Bode spectra of T700/VE composite in 3.5% NaCl solution. (a) Impedance modulus; (b) Phase angle.

The impedance data were fitted using the equivalent circuit models in Figure 3 [15,16]. The variations of the fitting parameters were analyzed. The constant phase angle element (Q) was used to simulate the non-ideal capacitance behavior of the composite electrode. In the models, R_s represents the solution resistance; Q_c and R_{p0} represent the information at

the interface between polymer and moisture, which is the constant phase angle element and the pore resistance of the matrix polymer due to the penetration of electrolyte from the surface through the defects to the fibers, respectively; Q_{dl} and R_{ct} represent the impedance behavior of the interface between carbon fibers and moisture, which is the double layer capacitance and the charge transfer resistance related to electrochemical reactions, respectively. Model A was applied in the initial stage (0–39 d). Model B was applied in the data fitting after the electrolyte penetrated the surface of carbon fibers with the time extended (40–205 d). Table 2 lists the EIS fitting parameters of the T700/VE composite specimen.

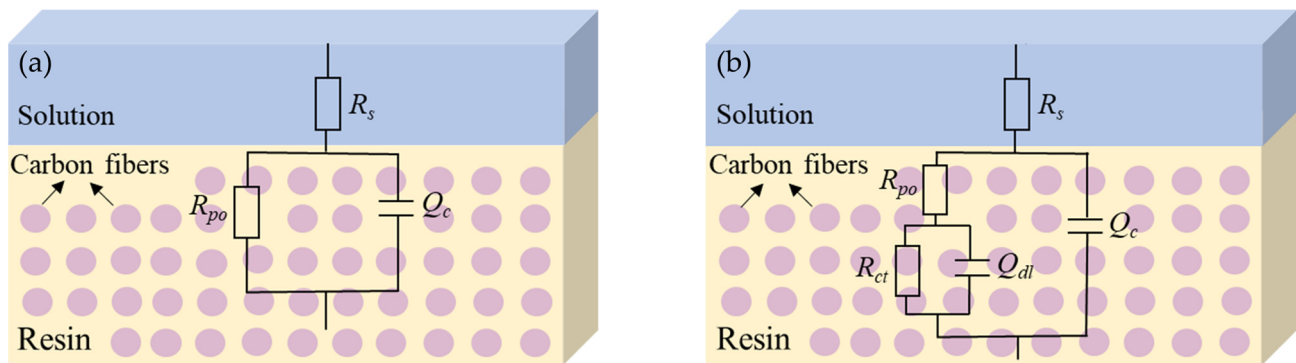


Figure 3. Equivalent circuit models used for EIS data fitting. (a) Model A; (b) Model B.

Table 2. The impedance fitting parameters of the T700/VE composite.

Time	R_s ($\Omega \text{ cm}^2$)	R_{po} ($\Omega \text{ cm}^2$)	Q_c ($\Omega^{-1} \text{ s}^n \text{ cm}^{-2}$)	n_{Qc}	R_{ct} ($\Omega \text{ cm}^2$)	Q_{dl} ($\Omega^{-1} \text{ s}^n \text{ cm}^{-2}$)	n_{Qdl}
5 min	4.177	6.09×10^6	2.06×10^{-5}	0.8990			
5 h	4.209	1.30×10^7	2.24×10^{-5}	0.8889			
10 d	3.128	8.09×10^6	3.43×10^{-5}	0.8444			
30 d	2.886	2.01×10^6	4.38×10^{-5}	0.8375			
43 d	2.267	1.56×10^6	4.05×10^{-5}	0.8457	9.19×10^6	6.87×10^{-6}	0.4170
58 d	3.277	3.41×10^5	4.57×10^{-5}	0.8292	1.99×10^6	7.61×10^{-6}	0.8504
91 d	1.593	2.87×10^5	5.08×10^{-5}	0.8337	2.48×10^5	4.44×10^{-5}	0.8543
133 d	1.655	1.07×10^5	6.09×10^{-5}	0.8113	2.05×10^5	8.93×10^{-5}	0.8999
163 d	2.586	1.20×10^5	6.38×10^{-5}	0.7900	2.22×10^5	3.56×10^{-5}	0.8129
205 d	1.962	1.30×10^5	4.61×10^{-5}	0.8437	5.37×10^5	4.04×10^{-5}	0.6064

Usually, the changes in the capacitance and resistance of polymer material can reflect the permeation of electrolytes within the polymer resin and the changes in the polymer's barrier property. Figure 4 shows the variations of Q_c and R_{po} of the resin matrix as a function of time. It can be seen that the Q_c increases rapidly during the initial immersion and then gradually increases, while the R_{po} decreases at first and then remains relatively stable after 120 d of immersion. The percentage mass change ($M/\%$) of the composite with time obtained by the weight gain test is also presented in Figure 4. It is seen that the variation trend of the M is in good consistent with that of the Q_c , demonstrating a fast increase in the moisture uptake during the first 6 d immersion and then a gradually decreasing absorption rate with time. It can be noticed that the percentage mass change of the composite in 205 d of immersion is very small—less than 0.4% of the original value of the specimen. This value is very close to the reported data for carbon fiber-reinforced vinyl ester composites in seawater in the literature [7,35]. This again demonstrates that the vinyl ester-based composites possess very good stability and durability in salt water. A comparison among the mass change ($M/\%$), the capacitance element (Q_c), and the pore resistance (R_{po}) show that the variation tendency of the M with time is well consistent with that of the Q_c and converse with that of the R_{po} . This is because the dielectric constant of

water (76.6–80.2) is much bigger than those of polymers (2.1–12.2) [14]. The water uptake of the polymer resin leads to an increase in the permittivity of the composite material, and therefore, the capacitance would be increased [36]. Meanwhile, the water uptake increases the ion conductivity of the material and thereby decreases the resistance. Comparing the variations of the Q_c and the R_{po} , it can be noticed that the variation amplitude of Q_c is less than half order of magnitude (from $2.06 \times 10^{-5} \Omega^{-1} \text{s}^n \text{cm}^{-2}$ to $4.61 \times 10^{-5} \Omega^{-1} \text{s}^n \text{cm}^{-2}$), while the variation amplitude of R_{po} is more than one and a half orders of magnitude (from 6.09×10^6 to $1.30 \times 10^5 \Omega \text{cm}^2$), which is much bigger than the variation amplitude of Q_c . So, the R_{po} might be a more suitable parameter to evaluate the performance of the composites, which changes more sensitively with water absorption. This is consistent with the literature [16], in which the authors thought that the pore resistance could possibly be a measure of the physical damage to the carbon fiber-reinforced composite.

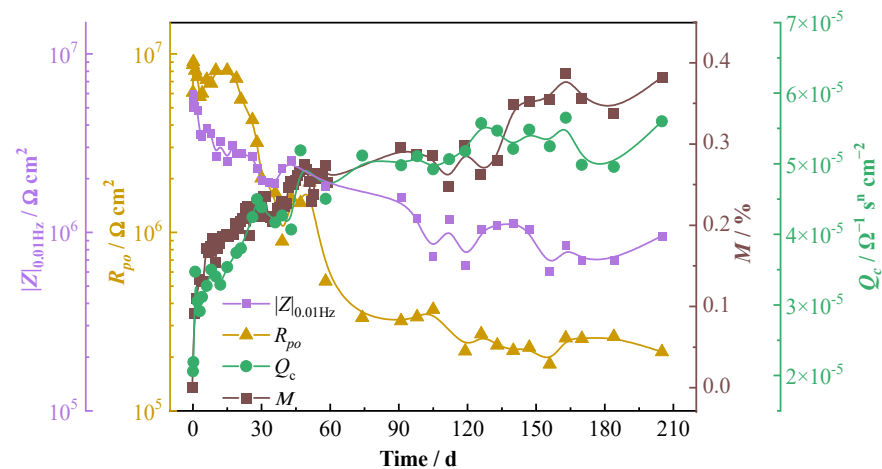


Figure 4. Variations of the percentage mass change, resin capacitance and resistance, and low-frequency impedance of T700/VE specimen with time.

The impedance $|Z|_{0.01\text{Hz}}$ is a parameter, which can be obtained without fitting and analyzing the impedance spectra, so it is often used to estimate the barrier property of coating materials instead of the resistance R_{po} . The curve of $|Z|_{0.01\text{Hz}}$ with immersion time is also presented in Figure 4. It can be seen that though the value of $|Z|_{0.01\text{Hz}}$ is lower than that of the R_{po} in the beginning and becomes higher in the later immersion period, it is obvious that, similar to the R_{po} , the variation trend of $|Z|_{0.01\text{Hz}}$ is also converse with that of the mass change ($M/\%$). When the water absorption percentage of the composite increases rapidly, the value of $|Z|_{0.01\text{Hz}}$ decreases quickly, and when the variation of the water absorption becomes smaller, the decreasing rate of the $|Z|_{0.01\text{Hz}}$ becomes slower. Thus, there is some correlation between the $|Z|_{0.01\text{Hz}}$ and the performance change of the carbon fiber-reinforced composites.

3.2. SEM-EDS and Bending Test Results of 700/VE Composite

Figure 5 shows the surface and cross-section morphologies of the 700/VE composite before and after immersion in 3.5% NaCl solution by SEM measurement. Before immersion, the surface is clean (Figure 5a), and the interface between the carbon fiber and resin matrix is intact (Figure 5b). The main elements detected by EDS are C (86.05 wt%), O (6.26 wt%), and N (7.33 wt%). After 205 d of immersion, most areas of the composite maintain integrity in microstructure; only signs of slight damage were observed in a few local areas, which is manifested by the dissolution of some polymer resin and interfacial regions broken between fibers and resin (Figure 5c,d). It also can be noticed that some white precipitates are covered on the surface of the specimen. The composition analysis of the white precipitates (shown in yellow square in Figure 5c) shows that except for the C (51.36 wt%), O (13.35 wt%), and N (0.89 wt%) elements, there are a certain amount of Na (10.34 wt%), Cl (10.52 wt%), and small amounts of Ca (4.99 wt%), Fe (3.46 wt%), K (1.56 wt%), Mg (1.34 wt%), and Si (0.73 wt%)

detected. This suggests that the precipitates may come from solution precipitation or the degradation product of the resin.

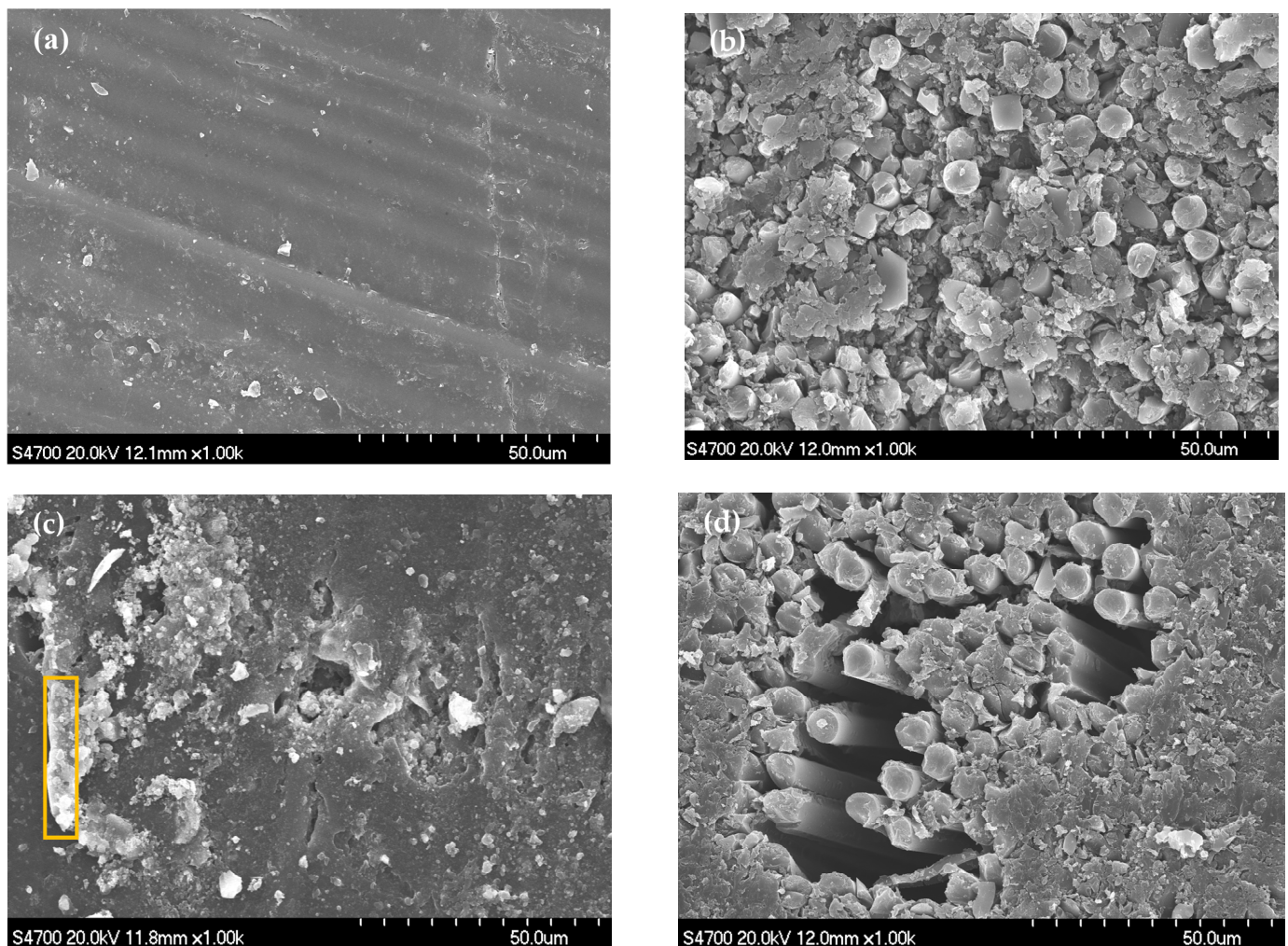


Figure 5. SEM images of the 700/VE specimen. (a,b) before immersion; (c,d) 205 d of immersion.

Table 3 shows the flexural modulus (E_f) results obtained from four-point bending tests for the T700/VE composite specimens before and after immersion in 3.5% NaCl solution at different times. From 0–60 d, the values of E_f experience a slight increase, but the overall changes are very small. However, as the electrolyte further penetrates into the composite, the value of E_f decreases significantly, which is 129 GPa and 123 GPa after 130 d and 205 d of immersion, respectively. Compared with the initial value of 740 GPa, the decreasing amplitude of the E_f is 82.5% and 83.4%, respectively. This is because that after water is absorbed, the polymer matrix becomes softer, which will cause debonding to occur at the fiber–matrix interface, therefore decreasing the adhesion force [2,8]. The fibers are not able to contribute well to the load transfer between the fibers and the matrix, therefore resulting in a decrease in the bending property of specimens.

Table 3. E_f results of T700/VE composite specimens after immersion at different times.

	Before Immersion	30 d	60 d	130 d	205 d
E_f /GPa	740	764	754	129	123
Reduction of E_f		−3.3%	−1.9%	82.5%	83.4%
$ Z _{0.01\text{Hz}}/\Omega \text{ cm}^2$	5.7×10^6	1.9×10^6	1.8×10^6	1.1×10^6	9.6×10^5
Reduction of $ Z _{0.01\text{Hz}}$		66.7%	68.4%	80.7%	83.2%

Table 3 also shows the value and the reduction of the $|Z|_{0.01\text{Hz}}$ at the same time as E_f measured. Comparing with the results of the EIS and bending tests, it is noted that the flexural modulus of the T700/VE specimen experiences no big change before 60 d but a significant decrease after 205 d of long-time immersion. The $|Z|_{0.01\text{Hz}}$ curve in Figure 4 shows a fast decrease at first and then towards a stable state after about 90 d. The decreasing magnitude of the $|Z|_{0.01\text{Hz}}$ at 130 d and 205 d is 80.7% and 83.2%, respectively, which is very close to that of flexural modulus (82.5% and 83.4%) at the same time. The data in Table 3 also show that compared with the four-point bending test, the EIS test is a more sensitive method for evaluating the performance of the carbon fiber-reinforced composite, especially in the early stage because the bending test is a destructive method and the dispersion of the data is relatively large. So, as a non-destructive method, EIS technology is more suitable for evaluating the degradation and performance of carbon fiber-reinforced composite materials. It is worth mentioning that there might be some relationship existing between the results of the bending test and the EIS test, which needs more study to be carried out in future work.

3.3. Evaluation of Degradation Performance of T700/VE Composites by Phase Angles in Middle Frequency

Our previous work suggested that the measurement of the phase angles in the middle–frequency range can be used to quickly evaluate the protection performance of organic coating on the metal substrate because a high correlation is found between the phase angles in the middle range and the impedance $|Z|_{0.01\text{Hz}}$ [26,27]. Since the phase angle is obtained in the middle-frequency range, it takes a very short time when measuring and is very suitable for rapid detection and evaluation in field application. Pearson’s correlation coefficient (r) is often used to evaluate the strength of a linear relationship between two variables. The closer the coefficient is to +1 or −1, the stronger the linear correlation. A positive value denotes a positive linear correlation and a negative value negative linear correlation. It is generally considered that $r \geq 0.7$ represents a strong correlation, and $r \geq 0.9$ is a very strong correlation [27,37,38]. In this study, Pearson correlation analysis was utilized to analyze the correlation between the variation of phase angles at different frequencies and that of the $|Z|_{0.01\text{Hz}}$ with time for the T700/VE composite. Table 4 presents the obtained r values in a certain frequency range. It was found that in the frequency range of 0.01–23.9 Hz, the values are higher than 0.75, which demonstrates that a strong correlation exists between the variation of phase angle in 0.01–23.9 Hz and the $|Z|_{0.01\text{Hz}}$. The phase angles in the frequency range (0.1 Hz, 0.85 Hz, 4.52 Hz, and 7.9 Hz) that the r higher than 0.9 was selected and the linear relation curve between phase angles and the $|Z|_{0.01\text{Hz}}$ was fitted by the Origin software. The results are shown in Figure 6, which denotes a very good linear relationship between the phase angle at each frequency selected with the logarithm of $|Z|_{0.01\text{Hz}}$. Since measuring in certain middle-frequency domains takes a much shorter time compared with that in low-frequency domains, it is suitable for fast testing and evaluating for field applications. So, for the T700/VE carbon fiber-reinforced polymer composite, the phase angles in a certain middle-frequency range, such as 1 to 10 Hz, may be used to rapidly detect and evaluate its performance and degradation, just like for evaluating the organic coatings performance [26,27].

Table 4. Pearson’s correlation coefficient (r) between the phase angles and $|Z|_{0.01\text{Hz}}$ for T700/VE.

Frequency/Hz	0.01	0.1	0.85	4.52	7.9	13.7	23.9	127	1172	10,826
r	0.88	0.95	0.95	0.94	0.90	0.86	0.75	0.10	−0.31	−0.6

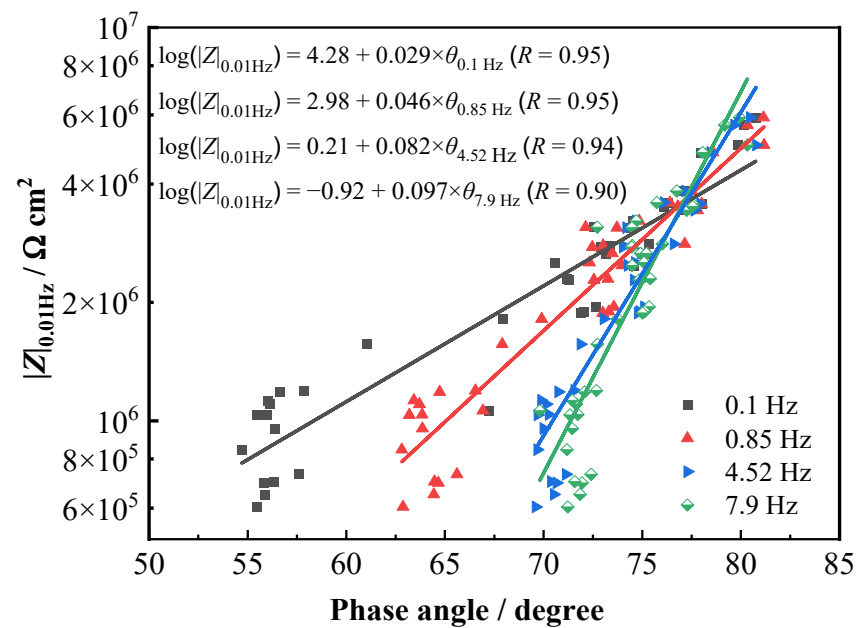


Figure 6. Fitting results of $|Z|_{0.01\text{ Hz}}$ and several phase angles in middle-frequency range for T700/VE composite.

The breakpoint frequency (f_b) was extracted from the Bode phase plot in Figure 2, and the variation of f_b with time is shown in Figure 7. It can be seen that f_b changes slightly with the testing time, fluctuating mainly in the range of 3.5×10^3 Hz and 1.1×10^4 Hz. It was reported in the literature that, for the polymer-coated metal system with coating degradation, the f_b shifts to larger values. When it reaches a value higher than 10^2 Hz (marked as the red horizontal line in Figure 7), visual corrosion occurs under the organic coating [22,25]. However, the result in Figure 8 indicates that for the studied T700/VE composite, the value of f_b varies with no big change and keeps higher than 10^2 Hz during the whole immersion period. This means that the f_b method is not suitable for monitoring the degradation of carbon fiber-reinforced polymer composite, which is consistent with the report by Alias et al. in the study of two other carbon fiber composites [15]. For the metals coated with organic coatings, in the degradation process of organic coatings, a good correlation exists between the f_b frequency in the high-frequency domain and the coating delamination area on metals; therefore, the degree of the coating deterioration can be obtained from measuring the f_b frequency. In the Bode phase plot, the phase angle maxima usually shift to higher frequencies with testing time for the coated metals. However, it is noticed that in the Bode phase plot of the T700/VE composite (Figure 2), there is almost no obvious change in the high-frequency range, probably because of its lack of micro-cracks as continuous diffusion channels through the thickness of the specimen as an organic coating [36]. So, the f_b method is not suitable for monitoring the degradation of carbon fiber-reinforced polymer composites.

3.4. EIS spectra of T700/BMI Composite and Degradation Performance Evaluation by Phase Angles in Middle Frequency

Figure 8 shows the Bode spectra of the T700/BMI composite immersion in 3.5% NaCl solution. Similar to the spectra of the T700/VE specimen, the spectra also present no big change after a long time. At 219 d of immersion, the value of $|Z|_{0.01\text{ Hz}}$ reaches $1.9 \times 10^6 \Omega \text{ cm}^2$ with a decrease of half order of magnitude compared with the initial value ($7.1 \times 10^6 \Omega \text{ cm}^2$), and the phase angle at 0.01 Hz frequency is as high as 60 degrees. These demonstrate that the T700/BMI composite has very good durability in 3.5% NaCl solution under open circuit potential conditions.

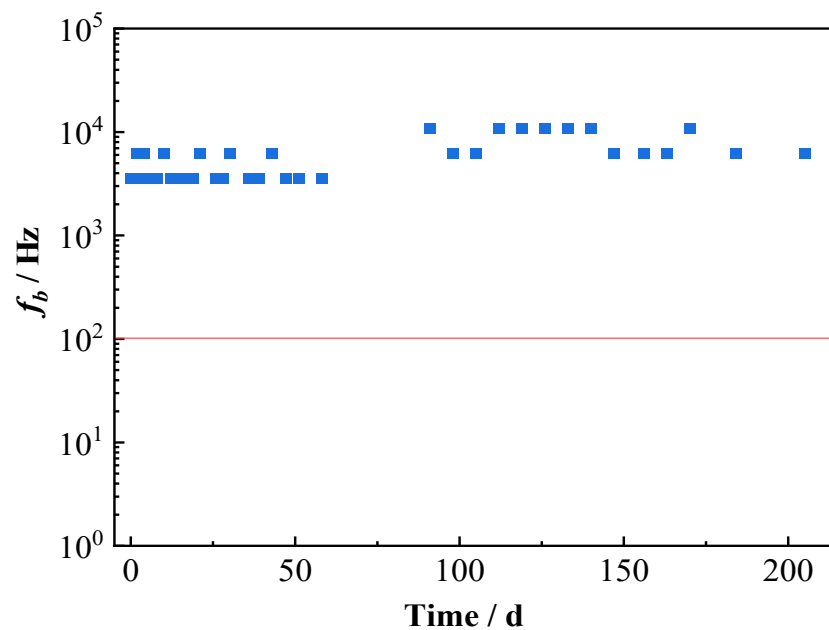


Figure 7. Variation of f_b with time for T700/VE composite specimen.

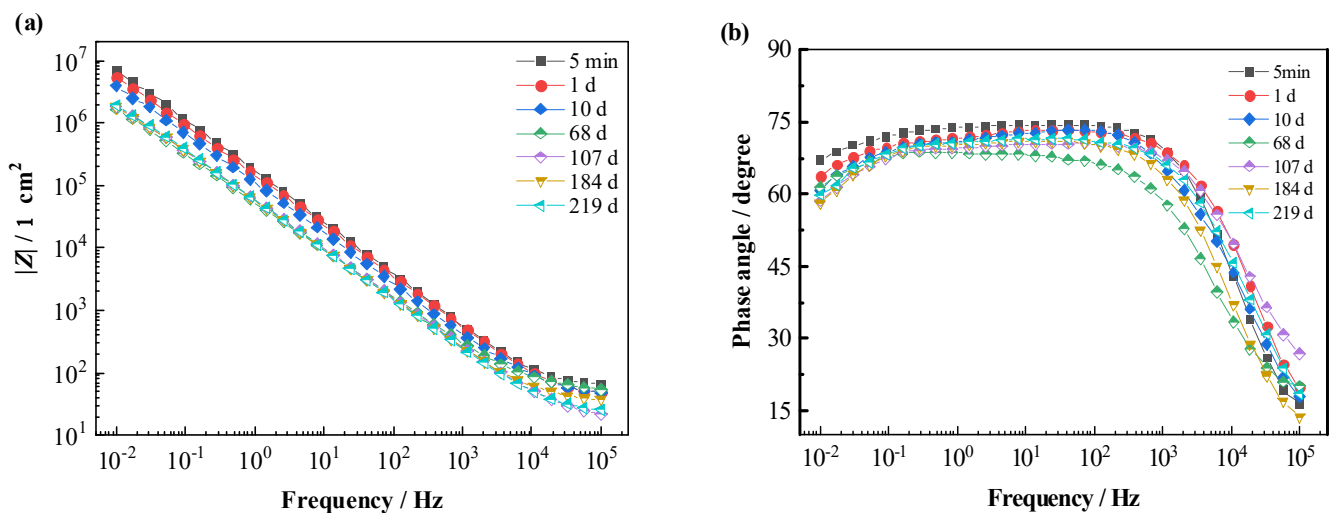


Figure 8. EIS Bode spectra of T700/BMI composite in 3.5% NaCl solution. (a) Impedance modulus; (b) Phase angle.

The impedance data in Figure 8 were fitted by the equivalent circuit models in Figure 3, and the EIS fitting parameters are shown in Table 5. The changes of the constant phase angle element Q_{po} and the pore resistance R_{po} with the time of the T700/BMI composite are presented in Figure 9, in which the impedance $|Z|_{0.01\text{Hz}}$ and the percentage mass change ($M/\%_t$) of the composite by weight gain test are also shown. Similar to the T700/VE composite, the $M/\%$ of the T700/BMI composite after 219 d of immersion is also very small, which is about 0.45% of the original value. It can be seen that the variation tendency of $M/\%$ with time is well consistent with that of the capacitance element Q_{po} and converse with that of the resistance R_{po} and impedance $|Z|_{0.01\text{Hz}}$. This verifies that the behavior of EIS electrochemical parameters, such as Q_{po} , R_{po} , and $|Z|_{0.01\text{Hz}}$, has a good relationship with that of the water adsorption for the T700/BMI composite. This is in good consistency with the results of the T700/VE composite.

Table 5. The impedance fitting parameters of the T700/BMI composite.

Time	R_s ($\Omega \text{ cm}^2$)	R_{po} ($\Omega \text{ cm}^2$)	Q_c ($\Omega^{-1} \text{ s}^n \text{ cm}^{-2}$)	n_{Qc}	R_{ct} ($\Omega \text{ cm}^2$)	Q_{dl} ($\Omega^{-1} \text{ s}^n \text{ cm}^{-2}$)	n_{Qdl}
5 min	59.52	4.40×10^7	1.28×10^{-6}	0.8259			
1 d	41.51	2.85×10^7	1.56×10^{-6}	0.8074			
10 d	44.17	1.63×10^7	2.11×10^{-6}	0.8014			
30 d	87.7	1.06×10^7	2.43×10^{-6}	0.7924			
37 d	66.22	1.19×10^7	2.56×10^{-6}	0.7983	4.05×10^7	2.61×10^{-7}	0.8309
68 d	52.07	1.50×10^7	4.57×10^{-6}	0.7574	8.26×10^6	4.10×10^{-6}	0.7612
107 d	17.84	6.90×10^6	4.00×10^{-6}	0.7825	4.77×10^6	5.93×10^{-6}	0.8090
149 d	24.42	5.71×10^6	4.63×10^{-6}	0.7718	1.17×10^6	4.55×10^{-6}	0.7969
184 d	35.08	5.74×10^6	4.00×10^{-6}	0.7911	1.16×10^6	6.68×10^{-6}	0.9584
219 d	22.76	7.04×10^6	3.91×10^{-6}	0.7940	1.65×10^6	6.76×10^{-6}	0.8740

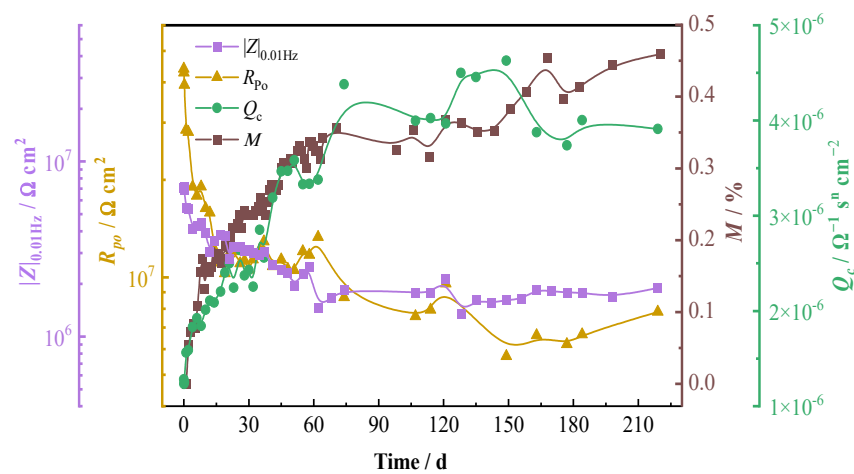


Figure 9. Variations of the percentage mass change, resin capacitance and resistance, and low-frequency impedance of T700/ BMI specimen with time.

The correlation between the variation of phase angles at various frequencies and the $|Z|_{0.01\text{Hz}}$ with testing time for the T700/5428 composite was analyzed by Pearson’s correlation coefficient (r) too. Table 6 presents the obtained r values. Similar to the above result of the T700/VE composite, a strong correlation ($r > 0.7$) was found to exist between the variation of phase angle in the 0.01–23.9 Hz frequency range and that of the $|Z|_{0.01\text{Hz}}$. Figure 10 shows the fitting results of the linear relation curve between the $|Z|_{0.01\text{Hz}}$ and the phase angles in 0.1–10 Hz frequency (0.1 Hz, 0.85 Hz, 4.52 Hz, and 7.9 Hz) by the Origin software. It is clear that a very good linear relationship exists between the logarithm of $|Z|_{0.01\text{Hz}}$ and the phase angles. The results of the T700/5428 composite are in good agreement with those of the T700/VE composite, confirming again that the values of phase angles in a certain middle frequency may be suggested to monitor the degradation of carbon fiber-reinforced polymer composites in engineering applications.

Table 6. Pearson’s correlation coefficient (r) between the phase angles and $|Z|_{0.01\text{Hz}}$ for T700/BMI.

Frequency/Hz	0.01	0.1	0.85	4.52	7.9	13.7	23.9	127	1172	10,826
r	0.92	0.89	0.95	0.94	0.91	0.86	0.78	0.40	0.08	−0.06

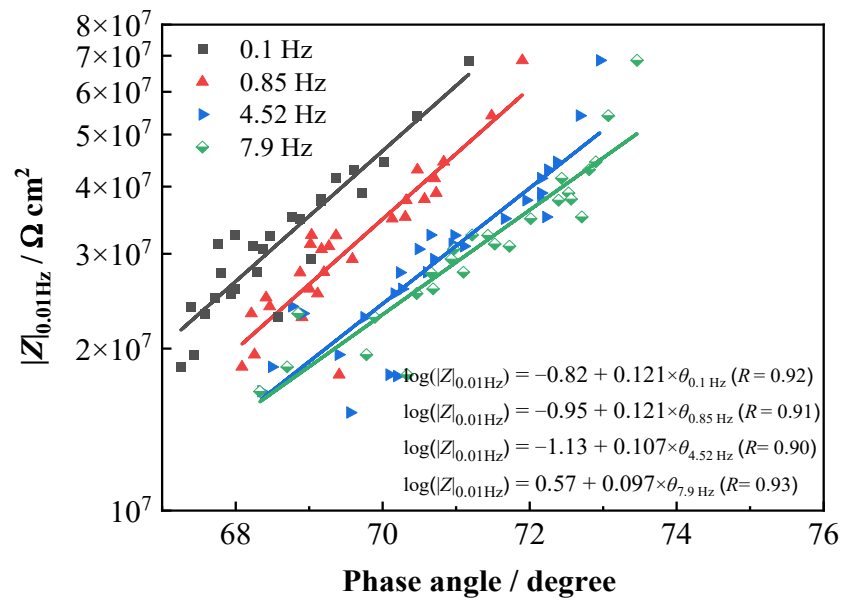


Figure 10. Fitting results of $|Z|_{0.01\text{Hz}}$ and several phase angles in middle-frequency range for T700/BMI specimen.

Because the measurement in lower frequency takes longer time than that in higher frequency, in terms of the need for rapid detection in field applications, it is suggested to use that testing of the phase angle around 10 Hz ($\theta_{10\text{Hz}}$) to evaluate the performance of the carbon fiber-reinforced polymer composites instead of testing the low-frequency impedance ($|Z|_{0.01\text{Hz}}$). Figure 11 shows the variations of $|Z|_{0.01\text{Hz}}$ and the phase angle at 10 Hz ($\theta_{10\text{Hz}}$) with testing time for two carbon fiber-reinforced polymer composites. For each composite material, the curve of $\theta_{10\text{Hz}}$ shows a very similar decreasing tendency to that of the $|Z|_{0.01\text{Hz}}$. That is, the phase angle at 10 Hz ($\theta_{10\text{Hz}}$) shows a high correlation with the $|Z|_{0.01\text{Hz}}$. Therefore, $\theta_{10\text{Hz}}$ could be suggested to quickly detect and evaluate the performance of carbon fiber-reinforced polymer composites in 3.5% NaCl immersion.

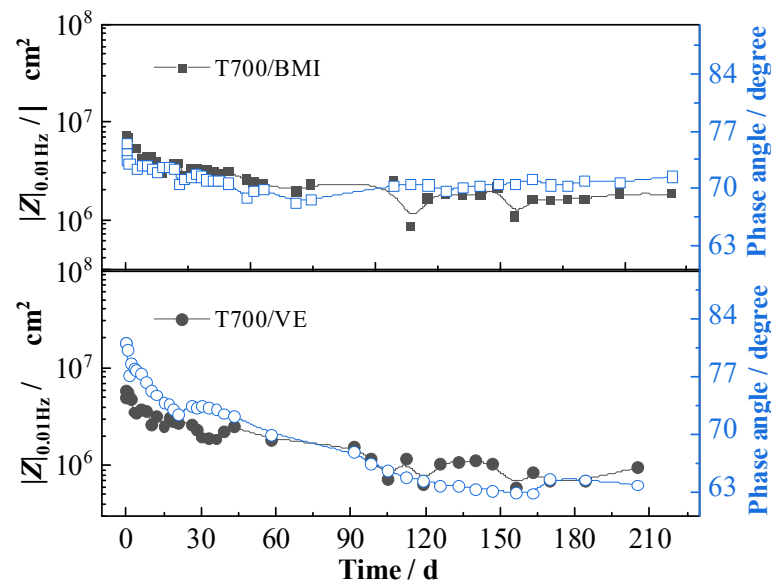


Figure 11. Variations of phase angle at 10 Hz and $|Z|_{0.01\text{Hz}}$ with testing time for two composites.

4. Conclusions

The performance of T700/VE and T700/BMI carbon fiber-reinforced polymer composites in 3.5% NaCl solution for long-time immersion was investigated by the electrochemical

impedance spectroscopy, weight gain test, combined with bending test and scanning electron microscope. Both composites have very good chemical stability under the natural immersion state, manifesting no big change in the EIS spectra, a small amount of water uptake (percentage mass change ($M/\%$) less than 0.5%), and good integrity in microstructure under electron microscope observation. However, the slight damage to the fiber/resin interface in local areas results in a significant decrease on the flexural modulus (around 84%). The variation of the moisture absorption percentage by weight gain test shows good consistency with that of the resin capacitance (Q_c), the resin resistance (R_{po}), and the low-frequency impedance ($|Z|_{0.01\text{Hz}}$). The measurement of the phase angles in the middle-frequency range was first applied to evaluate the performance of carbon fiber-reinforced polymer composites. There is a good linear relationship between the variations of phase angles in 0.1–10 Hz frequency range and the $|Z|_{0.01\text{Hz}}$. In terms of the need for rapid testing in field applications, it is suggested that the phase angle at 10 Hz ($\theta_{10\text{Hz}}$) might be suitable to evaluate the performance of the composites instead of the low-frequency impedance, which also needs further verification in more composites materials in future work. The f_b method is not suitable for monitoring the degradation of carbon fiber-reinforced polymer composites. The traceability relationship between the bending test and EIS test results needs more study to be carried out in future work.

Author Contributions: Writing—original draft preparation and investigation, H.Z. and F.K.; methodology and formal analysis, Y.D. and X.C.; investigation, Q.C.; supervision, writing—review and editing, Y.T.; writing—review and editing, X.Z. and Y.Z. All authors have read and agreed to the published version of the manuscript.

Funding: This research received no external funding.

Institutional Review Board Statement: Not applicable.

Informed Consent Statement: Not applicable.

Data Availability Statement: Not applicable.

Conflicts of Interest: The authors declare no conflict of interest.

References

1. Sloan, F.E.; Talbot, J.B. Corrosion of graphite-fiber-reinforced composites I—Galvanic coupling damage. *Corrosion* **1992**, *48*, 830–838. [[CrossRef](#)]
2. Selzer, R.; Friedrich, K. Mechanical properties and failure behaviour of carbon fibre-reinforced polymer composites under the influence of moisture. *Compos. Part A Appl. Sci. Manuf.* **1997**, *28*, 595–604. [[CrossRef](#)]
3. Antunes, R.A.; Lopes de Oliveira, M.C.; Ett, G. Investigation on the corrosion resistance of carbon black–graphite–poly(vinylidene fluoride) composite bipolar plates for polymer electrolyte membrane fuel cells. *Int. J. Hydrogen Energy* **2011**, *36*, 12474–12485. [[CrossRef](#)]
4. Ofoegbu, S.U.; Ferreira, M.G.S.; Zheludkevich, M.L. Galvanically stimulated degradation of carbon-fiber reinforced polymer composites: A critical review. *Materials* **2019**, *12*, 651. [[CrossRef](#)] [[PubMed](#)]
5. Zhu, J.; Wei, L.; Moahmoud, H.; Redaelli, E.; Xing, F.; Bertolini, L. Investigation on CFRP as dual-functional material in chloride-contaminated solutions. *Constr. Build. Mater.* **2017**, *151*, 127–137. [[CrossRef](#)]
6. Marouani, S.; Curtil, L.; Hamelin, P. Ageing of carbon/epoxy and carbon/vinylester composites used in the reinforcement and/or the repair of civil engineering structures. *Compos. Part B Eng.* **2012**, *43*, 2020–2030. [[CrossRef](#)]
7. Kootsookos, A.; Mouritz, A.P. Seawater durability of glass- and carbon-polymer composites. *Compos. Sci. Technol.* **2004**, *64*, 1503–1511. [[CrossRef](#)]
8. Afshar, A.; Liao, H.T.; Chiang, F.; Korach, C.S. Time-dependent changes in mechanical properties of carbon fiber vinyl ester composites exposed to marine environments. *Compos. Struct.* **2016**, *144*, 80–85. [[CrossRef](#)]
9. Alias, M.N.; Brown, R. Damage to composites from electrochemical processes. *Corrosion* **1992**, *48*, 373–378. [[CrossRef](#)]
10. Liu, S.; Chen, Y.; Chen, P.; Xu, D.; Xiong, X.; Wang, J. Properties of novel bismaleimide resins and thermal ageing effects on the ILSS performance of their carbon fibre–bismaleimide composites. *Polym. Compos.* **2019**, *40*, E1283–E1293. [[CrossRef](#)]
11. Akay, M.; Spratt, G.R.; Meenan, B. The effects of long-term exposure to high temperatures on the ILSS and impact performance of carbon fibre reinforced bismaleimide. *Compos. Sci. Technol.* **2003**, *63*, 1053–1059. [[CrossRef](#)]
12. Bao, L.R.; Yee, A.F. Effect of temperature on moisture absorption in a bismaleimide resin and its carbon fiber composites. *Polymer* **2002**, *43*, 3987–3997. [[CrossRef](#)]

13. Li, B.; Wen, Y.Y.; Wang, Q.Z.; Gu, Y.Z.; Li, M.; Zhang, Z.G. Hygrothermal mechanical properties of domestic carbon fiber/bismaleimide resin composites for aviation application. *J. Aeronaut. Mater.* **2020**, *40*, 80–87. [[CrossRef](#)]
14. Pavlacky, D.A.; Gelling, V.J.; Ulven, C.A. The use of electrochemical impedance spectroscopy to monitor delaminations in polymer matrix composites: A review. *Int. J. Mater. Sci.* **2011**, *1*, 23–29.
15. Alias, M.N.; Brown, R. Corrosion behavior of carbon fiber composites in the marine environment. *Corros. Sci.* **1993**, *35*, 395–402. [[CrossRef](#)]
16. Kaushik, D.; Alias, M.N.; Brown, R. An Impedance study of a carbon fiber/vinyl ester composite. *Corrosion* **1991**, *47*, 859–867. [[CrossRef](#)]
17. Taylor, S.R.; Wall, F.D.; Cahen, G.L. The detection and analysis of electrochemical damage in bismaleimide/graphite fiber composites. *J. Electrochem. Soc.* **1996**, *143*, 449. [[CrossRef](#)]
18. Mueller, Y.; Tognini, R.; Mayer, J.; Virtanen, S. Anodized titanium and stainless steel in contact with CFRP: An electrochemical approach considering galvanic corrosion. *J. Biomed. Mater. Res. Part A* **2007**, *82*, 936–946. [[CrossRef](#)]
19. Zhang, C.; Zheng, D.; Song, G.L.; Guo, Y.; Liu, M.; Kia, H. Effect of the microstructure of carbon fiber reinforced polymer on electrochemical behavior. *J. Electrochem. Soc.* **2018**, *165*, C647. [[CrossRef](#)]
20. Zhang, C.; Zheng, D.; Song, G.L.; Guo, Y.; Liu, M.; Kia, H. Influence of microstructure of carbon fibre reinforced polymer on the metal in contact. *J. Mater. Res. Technol.* **2020**, *9*, 560–573. [[CrossRef](#)]
21. McIntyre, J.M.; Pham, H.Q. Electrochemical impedance spectroscopy; a tool for organic coatings optimizations. *Prog. Org. Coat.* **1996**, *27*, 201–207. [[CrossRef](#)]
22. Hirayama, R.; Haruyama, S. Electrochemical impedance for degraded coated steel having pores. *Corrosion* **1991**, *47*, 952–958. [[CrossRef](#)]
23. Tsai, C.H.; Mansfeld, F. Determination of coating deterioration with EIS: Part II. Development of a method for field testing of protective coatings. *Corrosion* **1993**, *49*, 726–737. [[CrossRef](#)]
24. Mahdavian, M.; Attar, M.M. Another approach in analysis of paint coatings with EIS measurement: Phase angle at high frequencies. *Corros. Sci.* **2006**, *48*, 4152–4157. [[CrossRef](#)]
25. Feng, Z.; Frankel, G.S. Evaluation of Coated Al Alloy Using the Breakpoint Frequency Method. *Electrochim. Acta* **2016**, *187*, 605–615. [[CrossRef](#)]
26. Zuo, Y.; Pang, R.; Li, W.; Xiong, J.P.; Tang, Y.M. The evaluation of coating performance by the variations of phase angles in middle and high frequency domains of EIS. *Corros. Sci.* **2008**, *50*, 3322–3328. [[CrossRef](#)]
27. Fu, T.; Tang, X.; Cai, Z.; Zuo, Y.; Tang, Y.; Zhao, X. Correlation research of phase angle variation and coating performance by means of Pearson's correlation coefficient. *Prog. Org. Coat.* **2020**, *139*, 105459. [[CrossRef](#)]
28. Bing, L.; Xu, A.; Liang, Y.; Huang, Z.; Qiao, Z.; Xia, D.; Zhang, S.; Li, Z.; Zhang, F.; Chen, P. Evaluation on protective performance of organic coatings by analyzing the change rate of phase angle at high frequency. *Int. J. Electrochem. Sci.* **2012**, *7*, 8859–8868.
29. Xia, D.; Song, S.; Wang, J.; Bi, H.; Han, Z. Fast evaluation of degradation degree of organic coatings by analyzing electrochemical impedance spectroscopy data. *Trans. Tianjin Univ.* **2012**, *18*, 15–20. [[CrossRef](#)]
30. Nardeli, J.V.; Snihirova, D.V.; Fugivara, C.S.; Montemor, M.F.; Pinto, E.R.P.; Messaddecq, Y.; Benedetti, A.V. Localised corrosion assesment of crambe-oil-based polyurethane coatings applied on the ASTM 1200 aluminum alloy. *Corros. Sci.* **2016**, *111*, 422–435. [[CrossRef](#)]
31. Chen, Z.; He, Z.; Yu, F.; Wang, Y. Study and application of electrochemical impedance spectroscopy for quickly evaluating the performance of coatings and predicting the failure time in the development of waterborne epoxy micaceous iron oxide coatings. *Int. J. Electrochem. Sci.* **2017**, *12*, 2798–2812. [[CrossRef](#)]
32. Cai, G.; Wang, H.; Jiang, D.; Dong, Z. Impedance sensor for the early failure diagnosis of organic coatings. *J. Coat. Technol. Res.* **2018**, *15*, 1259–1272. [[CrossRef](#)]
33. Fan, C.; Shi, J.; Dilger, K. Water uptake and interfacial delamination of an epoxy-coated galvanized steel: An electrochemical impedance spectroscopic study. *Prog. Org. Coat.* **2019**, *137*, 105333. [[CrossRef](#)]
34. Tang, Y.; Hartt, W.; Granata, R.; Yu, H.; Farooq, M.U. Degradation of carbon/vinyl ester composites under cathodic polarization in seawater. *J. Compos. Mater.* **2012**, *46*, 3115–3120. [[CrossRef](#)]
35. Mahfuz, H.; Powell, F.; Granata, R.; Hosur, M.; Khan, M. Coating of Carbon Fiber with Polyhedral Oligomeric Silsesquioxane (POSS) to Enhance Mechanical Properties and Durability of Carbon/Vinyl Ester Composites. *Materials* **2011**, *4*, 1619–1631. [[CrossRef](#)]
36. Fazzino, P.D.; Reifsnider, K.L.; Majumdar, P. Impedance spectroscopy for progressive damage analysis in woven composites. *Compos. Sci. Technol.* **2009**, *69*, 2008–2014. [[CrossRef](#)]
37. Montazeri, S.; Ranjbar, Z.; Rastegar, S.; Deflorian, F. A new approach to estimates the adhesion durability of an epoxy coating through wet and dry cycles using creep-recovery modeling. *Prog. Org. Coat.* **2021**, *159*, 106442. [[CrossRef](#)]
38. Choi, S.; Choi, J.; Park, C. Multivariate analysis-based laser-induced breakdown spectroscopy for monitoring of laser paint cleaning. *Appl. Phys. B* **2023**, *129*, 8. [[CrossRef](#)]

Disclaimer/Publisher's Note: The statements, opinions and data contained in all publications are solely those of the individual author(s) and contributor(s) and not of MDPI and/or the editor(s). MDPI and/or the editor(s) disclaim responsibility for any injury to people or property resulting from any ideas, methods, instructions or products referred to in the content.